

Structure and conductance of a gold atomic chain

Masakuni Okamoto

Takayanagi Particle Surface Project, ERATO, Japan Science and Technology Corporation, 2-13-3 Akebono, Tachikawa, Tokyo 190-0012, Japan

Kunio Takayanagi

Department of Material Science and Engineering, Tokyo Institute of Technology, 4259 Nagatsuta, Midori-ku, Yokohama 226-8502, Japan

(Received 26 February 1999)

The conductances of linear chains of gold atoms suspended between two electrodes were calculated while the distance between the electrodes was increased. The stable structures of the linear chains of the gold atoms at low temperature were initially determined by using the *ab initio* local spin-density-functional approach. As the average bond length $\langle d \rangle$ increased, the spacings of the neighboring gold atoms modulated similarly to the Peierls transition. The maximum tensile force of a linear four-atom-chain was 0.91 nN and occurred at $\langle d \rangle \approx 3.1 \text{ \AA}$. The electric conductances were then calculated using the recursion transfer-matrix method. The calculation indicated that the conductance at the Fermi level of the modulated chain decreased from $1G_0$ ($=2e^2/h$) as the chain was stretched. [S0163-1829(99)06335-3]

Conductance quantization of metal nanowires is of particular interest because of their applications to future technologies. Nanowires exhibited conductances in steps of $G_0 = 2e^2/h$, where e is the electron charge and h is Planck's constant, at contacts made by scanning tunneling microscope (STM) geometry¹⁻⁴ and other methods.⁵⁻⁷ Conductances for a nanocontact or a nanowire were also theoretically calculated for Al,⁸⁻¹¹ Na,¹² Cu,¹³ Au,¹⁴ Ni,¹⁵ Nb,⁹ S,¹⁰ Xe,¹⁶ Si,¹⁷ and C (Ref. 18) by using the linear-response (Kubo) formula,⁸ the tight-binding approach,^{9,15} the density-functional Green-function approach,^{10,11,16-18} and the recursion transfer-matrix (RTM) method.¹²⁻¹⁴

The atomic chains of gold atoms were recently observed by an ultrahigh-vacuum (UHV) electron microscope.¹⁹ The conductance of the chains was measured during the withdrawal of an STM tip. That observation demonstrated that a single [110] atomic row chain had a conductance of $1G_0$. The single atomic row chain, which was formed in a [100] orientation by thinning from a gold film,²⁰ had anomalously large interatomic spacings of 3.5–4.0 Å. In another recent experiment using an STM configuration,²¹ the maximum lengths of the gold contacts at their rupturing point suggested an atom spacing of 3.6 Å for a single chain with a conductance of $1G_0$.

Theoretical studies on gold chains¹⁴ have specified $1G_0$ for a gold one-atom-row chain but offered no speculation on the extremely large interatomic spacings. The semiempirical potentials used to determine the structures were derived from the effective-medium theory (EMT),²² which is known to become less effective for low coordination systems, such as a one-dimensional chain.²³ In addition, the effects due to spins and electron correlations were not sufficiently estimated using the EMT potential calculation.

In this paper we report on the *ab initio* local spin-density-functional (LSDF) calculation for optimizing the structures of single-row gold atomic chains at low temperature, and the electric conductance for the chains between jellium electrodes, using the RTM method. Our result demonstrates that

a single-row gold atomic chain is modulated as it is stretched, similar to a Peierls transition. A linear chain with four atoms has a maximum restoring force of 0.91 nN at an average interatomic spacing of 3.1 Å. The interatomic distance of this chain reaches 3.45 Å, but the conductance is approximately $0.4 G_0$.

We calculated the electric conductance of a linear chain of gold atoms suspended between two electrodes using the model shown in Fig. 1. The linear chain was L long with n gold atoms (n -atom-chain) and connected to pyramidal clusters at both ends, similar to the [100] gold strand.¹⁹ We calculated the conductances for the chains of equal bond length and for the optimized structures. The optimized structure for a linear n -atom chain was determined approximately by replacing it with that of an $(n+2)$ -atom cluster (see the rectangular area in Fig. 1), and each bond length d_i between the i th and $(i-1)$ th atoms was determined using the *ab initio* LSDF approach; without any symmetry restriction applied, the cluster length was fixed to L . The localized numerical basis functions of the 6-31G** level and the exchange-

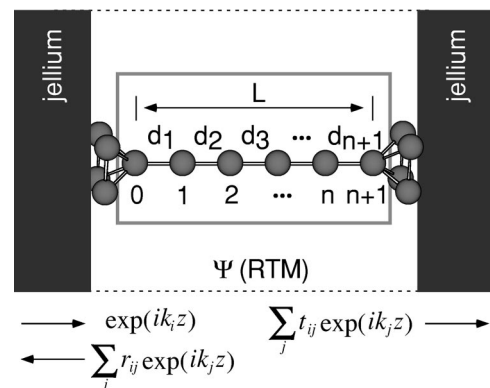


FIG. 1. Model for the gold n -atom chain used in this calculation. z axis is taken parallel to the chain direction. An incident electron $e^{ik_z z}$ is reflected $\sum_j r_{ij} e^{-ik_j z}$ or transmitted $\sum_j t_{ij} e^{ik_j z}$, and the total wave function is solved by the RTM algorithm.

correlation functional of Vosko, Wilk, and Nusair²⁴ and frozen-core approximation were used for optimization.

The electric conductance G at zero-bias voltage was calculated using the RTM method¹² in the form

$$G = \frac{2e^2}{h} \sum_{i,j} |t_{ij}|^2 \frac{k_j}{k_i}, \quad (1)$$

where k_i and k_j are z components of the wave numbers of electrons in the conduction channels i and j , and t_{ij} is the transmission matrix element. This derived expression is the same as the Landauer-Büttiker formula.²⁵

The effective potential, which causes the scattering of electrons, is calculated within the local-density approximation as

$$V_{eff}(\mathbf{r}) = \sum_{\mu} V_{ps}^{ion}(\mathbf{r} - \mathbf{R}_{\mu}) + \int d\mathbf{r}' \frac{\rho(\mathbf{r}')}{|\mathbf{r} - \mathbf{r}'|} + V_{xc}[\rho(\mathbf{r})], \quad (2)$$

where \mathbf{R}_{μ} is the position of the μ th atom, $\rho(\mathbf{r})$ is the valence electron density, V_{ps}^{ion} is the ionic part of a pseudopotential, and V_{xc} is the exchange-correlation potential. We adopted V_{xc} of the Ceperley-Alder form²⁶ as parametrized by Perdew and Zunger.²⁷ We neglected the contributions of the $5d$ electrons to the conductance; a local pseudopotential V_{ps}^{6s} of a gold $6s$ electron for V_{ps}^{ion} was constructed using the algorithm by Bachelet, Hamann, and Schlüter.²⁸ Since we only considered a local pseudopotential, the $6p$ pseudo-orbital energy becomes about 0.4 eV lower than the correct $6p$ energy level.

In the conductance calculation, the valence-electron density $\rho(\mathbf{r})$ was approximated by the sum of the $6s$ electron densities of the isolated atoms at \mathbf{R}_{μ} ,

$$\rho(\mathbf{r}) = \sum_{\mu} |\psi_{ps}^{6s}(\mathbf{r} - \mathbf{R}_{\mu})|^2, \quad (3)$$

and therefore, the electron density is not self-consistent with the effective potential.

The local charge neutrality for the metal contacts²⁹ is satisfied when the chain and the jellium electrodes in Fig. 1 have the same Fermi level. The Fermi level of the n -atom-chain is replaced by the value for the infinite chain, calculated by a band calculation within the same approximation as Eq. (3). The present approximation implicitly changes the work function of the jellium electrode, because the calculated Fermi level varies from -6.59 eV to -5.39 eV as the bond length changes from 2.6 Å to 3.4 Å. The Fermi energy of the jellium is kept constant at 5.53 eV.

We used a unit cell of 20 Å in the x and y directions with a periodic boundary condition. The xy grid used in the FFT had 128×128 points, and we used a recursion step length in the z direction of 0.5 Å. The conductance curves were converged for a plane-wave cutoff energy of 40 eV, corresponding to 341 channels. The conductance was averaged over four k points in the xy Brillouin zone. The conductance dispersion was very small (within $0.01 G_0$), which indicates that our xy unit cell was sufficiently large. A buffer layer

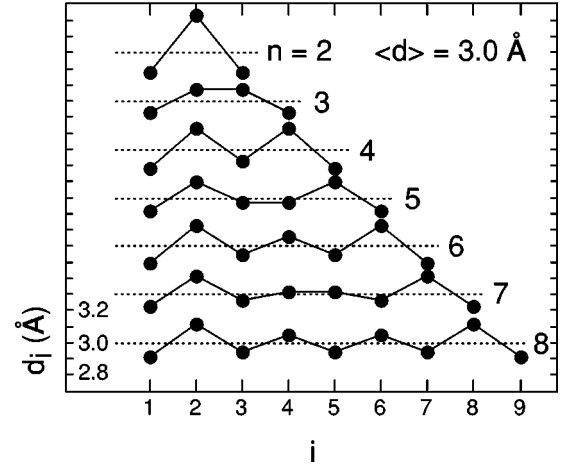


FIG. 2. Bond length d_i of the optimized n -atom chains for $i = 1, 2, \dots, n$ ($n = 1, 2, \dots, 8$) with $\langle d \rangle = 3.0$ Å at $T = 0$ K. Each broken line corresponds to 3.0 Å for each n .

3 -Å thick was inserted to smoothly connect the effective potential at the contact between the chain and the electrode.

The optimized structure for each of the n -atom-chains ($n = 1, 2, \dots, 8$) in Fig. 1 was calculated at $T = 0$ K as a function of the average bond length $\langle d \rangle$, defined as $\langle d \rangle \equiv L/(n+1)$. For an average bond length of 3.0 Å, the optimized bond lengths d_i ($i = 1, 2, \dots, n+1$) in each chain deviate from the average bond length, as shown in Fig. 2. We observed three characteristics of the structure. First, the bond lengths were symmetrical around the center of the chain. Second, the bond-length deviation was oscillating and was dumped from the edge toward the center of the chain. Finally, the *odd* number chains ($n = 1, 3, 5, 7$) had smaller amplitudes of the dumped oscillation than the *even* number chains ($n = 2, 4, 6, 8$), because of the destructive phase relation. The bond-length oscillations, e.g., those with an amplitude of 0.05 Å at the central part of the six-atom chain, were caused by a Peierls transition.³⁰ We calculated the stable structures of the stretched infinite-length chains using the first-principles pseudopotential band calculation. We used a cutoff energy of 13.86 Hartree, and the electronic states were calculated self-consistently. The bond-length oscillations became apparent for $\langle d \rangle > 2.8$ Å, while the equilibrium bond length was 2.6 Å. The oscillation amplitudes were 0.0 , 0.2 , and 0.4 Å for $\langle d \rangle = 2.8, 2.9$, and 3.0 Å.

The bond-length oscillations at the chain ends in Fig. 2 seemed to be an edge (surface state) effect. The cluster calculations were performed with pyramidal clusters at the ends. The calculation converged when the Fermi level was smeared to fit with the Fermi-Dirac distribution at temperature higher than 2700 K, and the force directions acting on each atom suggested dimerization (Peierls distortion), but with much less amplitude.

Figure 3(a) shows the change of d_i in the four-atom chain caused by stretching. Bond lengths d_1 (and d_5) and d_3 increased to their maximum values at about 2.9 Å at $\langle d \rangle = 3.0$ Å, reaching $d_{dimer} = 2.71$ Å for $\langle d \rangle > 3.5$ Å. Here, 2.71 Å is the bond length of an isolated gold dimer. The stretching chain thus changes its bonding nature from an atom-coupling state to a dimer-coupling state around $\langle d \rangle = 3.0$ Å.

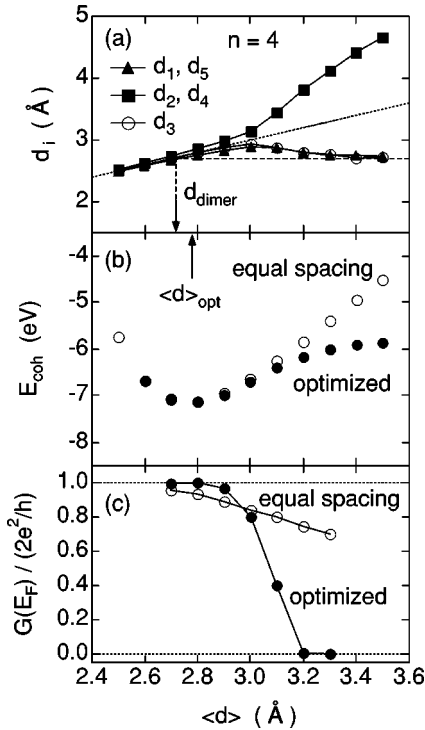


FIG. 3. Several calculated results as a function of the average bond length $\langle d \rangle$ for $n=4$ at $T=0$ K. (a) Bond lengths d_i ($i=1, 2, \dots, 5$). The calculated result is symmetric, $d_1=d_5$ and $d_2=d_4$. The broken line is a plot of $\langle d \rangle$ and $d_{dimer}=2.71$ Å. (b) Cohesive energies E_{coh}^{eq} (equal spacing) and E_{coh}^{opt} (optimized). The most stable lengths for the two cases are the same value $\langle d \rangle_{opt}=2.77$ Å. (c) Conductances at the Fermi level $G^{eq}(E_F)$ and $G^{opt}(E_F)$.

The cohesive energies calculated for the optimized chain E_{coh}^{opt} and for the equal spacing chain E_{coh}^{eq} demonstrate the increasing stability of the former structure as $\langle d \rangle$ increases [see Fig. 3(b)]. Their energy difference was only 0.051 eV at $\langle d \rangle=3.0$ Å, while it was 0.134 eV at $\langle d \rangle=3.1$ Å; therefore, the dimer-coupling state can appear even at room temperature. The restoring force given by $|dE_{coh}/dL|$ has a maximum, in relation to the bond-length change d_3 shown in Fig. 3(a). The maximum restoring force and the corresponding critical bond length were 0.91 nN and 3.1 Å for the optimized chain, and 1.39 nN at 3.2 Å. Therefore, both chains can break if they experience the maximum forces. The energy barrier which confines a dimer in a linear line is estimated by calculating the energy necessary to remove a gold dimer in a direction perpendicular to the chain axis. The energy barriers were found to be sufficiently large for the confinement, even at room temperature; 0.981 eV for $\langle d \rangle=3.1$ Å and 0.448 eV for $\langle d \rangle=3.2$ Å.

The conductances at the Fermi level are plotted as a function of $\langle d \rangle$ in Fig. 3(c) for the optimized and uniform chains of $n=4$. The conductance of the uniform chain decreased as the chain was stretched; this is an effect caused by poor potential continuity at the chain and the pyramidal cluster. The scattering (and interference) of the electrons due to the somewhat abrupt change in the potential reduces the conductance.³¹ This interference effect should be decreased or diminished when the potential is determined self-

consistently. We believe, therefore, that the equal-spaced chain has $1G_0$, independent of $\langle d \rangle$ until it breaks. In contrast, the conductance of the optimized chain keeps $1G_0$ for $\langle d \rangle$ shorter than 3.0 Å, but decreases for a longer $\langle d \rangle$ of the dimer-coupling state. The conductance was $0.4G_0$ for $\langle d \rangle=3.1$ Å, at which the chain had a maximum restoring force of 0.91 nN. This kind of decrease in the conductance is caused by dimerization or a Peierls-like transition of the stretched gold linear chain. Our band calculation for the infinite length chain, within the same approximation as for $\rho(\mathbf{r})$ in Eq. (3), shows energy gaps at the Fermi level. The energy gaps increased as $\langle d \rangle$ increased and were 0.149, 0.453, and 1.536 eV for the chains of $\langle d \rangle=2.8, 3.0,$ and 3.2 Å.

Our calculation for the optimized chain for $n=4$ was changed by stretching from an atom-coupling system to a dimer-coupling system. The transition started at $\langle d \rangle \approx 3.0-3.1$ Å, and the conductance started to decrease from $1G_0$. Around this transition, the stretching force reached a maximum value of 0.91 nN at $\langle d \rangle=3.1$ Å. These characteristics also hold for the chains for $n=2$ and $n=6$. In experiments with STM configurations, the force-tip displacement was proportional to its elasticity until it ruptured. The maximum force at the rupture in the literature³² was 1.5 ± 0.2 nN. The dimer-coupling system could not have been realized in these experiments because our calculation shows that strong stretching forces, exceeding 0.9 nN, easily break the chain before $\langle d \rangle$ reaches 3.1 Å. A recent low-temperature experiment for gold atom chains,²¹ which reported 3.6 Å as the maximum stretch of a bond before it breaks, is in accordance with our result. Our optimized chain of $\langle d \rangle=3.1$ Å has $d_1 (=d_5) \approx d_3 \approx 2.87$ Å and $d_2 (=d_4) \approx 3.45$ Å. The longest bond length, which is the breaking bond during stretching, is predicted to be 3.45 Å. The disagreement regarding conductance before the break is unsatisfactory; it was $1G_0$ in the experiment, but $0.4G_0$ in our calculation.

The present results do not provide a sound explanation for the report¹⁹ that a gold chain remains even at $\langle d \rangle=4.0$ Å. We considered three possible explanations. First, a neglected effect, such as heating of the electronic states by the electron beam in the microscope, might change the atom positions and the electron density profile. Second, the electron beam might charge the chain. Finally, although our LSDF calculations treated the electron-spin effect correctly, the approximation of the electron exchange-correlation energy might be less accurate for a long bond length. Therefore, we must investigate these effects in a self-consistent scheme or beyond a one-electron approximation.

In summary, we calculated the conductance of a linear chain of four gold atoms suspended between two electrodes, each of which had a pyramidal cluster at the apex. The conductance change caused by stretching the chain, calculated by the RTM method and a pseudopotential, exhibited a transition from a metallic conductance ($G=1G_0$) to an insulating one. The average bond length $\langle d \rangle$ at the transition was 3.0–3.1 Å, where the chain structure changed, caused by the stretching from an atom-coupling state to a dimer-coupling one. This structural transition was calculated using the *ab initio* LSDF approach. This structural transition appeared for

all the calculated chains consisting of 2, 3, 4, 5, 6, 7, and 8 atoms at low temperature. The dimer-coupling structures that appeared for a $\langle d \rangle$ exceeding 3.0 Å resembled a Peierls transition.

We would like to express thanks to Dr. H. Ohnishi and Dr. Y. Kondo for detailed discussions about their experimental data, and Professor M. Tsukada for many valuable and stimulating discussions.

-
- ¹N. Agraït, J. G. Rodrigo, and S. Vieira, *Phys. Rev. B* **47**, 12 345 (1993).
- ²J. I. Pascual, J. Méndez, J. Gómez-Herrero, A. M. Baró, N. García, Uzi Landman, W. D. Luedtke, E. N. Bogachek, and H.-P. Cheng, *Science* **267**, 1793 (1995).
- ³L. Olesen, E. Laegsgaard, I. Stensgaard, F. Besenbacher, J. Schiötz, P. Stoltze, K. W. Jacobsen, and J. K. Nørskov, *Phys. Rev. Lett.* **72**, 2251 (1994).
- ⁴J. L. Costa-Krämer, N. García, P. García-Mochales, P. A. Serena, M. I. Marqués, and A. Correia, *Phys. Rev. B* **55**, 5416 (1997).
- ⁵C. J. Muller, J. M. Krans, T. N. Todorov, and M. A. Reed, *Phys. Rev. B* **53**, 1022 (1996).
- ⁶Uzi Landman, W. D. Luedtke, B. E. Salisbury, and R. L. Whetten, *Phys. Rev. Lett.* **77**, 1362 (1996).
- ⁷H. Yasuda and A. Sakai, *Phys. Rev. B* **56**, 1069 (1997).
- ⁸R. N. Barnett and U. Landman, *Nature (London)* **387**, 788 (1997).
- ⁹J. C. Cuevas, A. L. Yeyati, and A. Martín-Rodero, *Phys. Rev. Lett.* **80**, 1066 (1998).
- ¹⁰N. D. Lang, *Phys. Rev. B* **52**, 5335 (1995).
- ¹¹C. C. Wan, J.-L. Mozos, G. Taraschi, J. Wang, and H. Guo, *Appl. Phys. Lett.* **71**, 419 (1997).
- ¹²K. Hirose and M. Tsukada, *Phys. Rev. B* **51**, 5278 (1995).
- ¹³H. Mehrez and S. Ciraci, *Phys. Rev. B* **56**, 12 632 (1997).
- ¹⁴M. R. Sørensen, M. Brandbyge, and K. W. Jacobsen, *Phys. Rev. B* **57**, 3283 (1998).
- ¹⁵A. M. Bratkovsky, A. P. Sutton, and T. N. Todorov, *Phys. Rev. B* **52**, 5036 (1995).
- ¹⁶A. Yazdani, D. M. Eigler, and N. D. Lang, *Science* **272**, 1921 (1996).
- ¹⁷J.-L. Mozos, C. C. Wan, G. Taraschi, J. Wang, and H. Guo, *Phys. Rev. B* **56**, R4351 (1997).
- ¹⁸N. D. Lang and Ph. Avouris, *Phys. Rev. Lett.* **81**, 3515 (1998).
- ¹⁹H. Ohnishi, Y. Kondo, and K. Takayanagi, *Nature (London)* **395**, 780 (1998).
- ²⁰Y. Kondo and K. Takayanagi, *Phys. Rev. Lett.* **79**, 3455 (1997).
- ²¹A. I. Yanson, G. Rubio Bollinger, H. E. van den Brom, N. Agraït, and J. M. van Ruitenbeek, *Nature (London)* **395**, 783 (1998).
- ²²K. W. Jacobsen, J. K. Nørskov, and M. J. Puska, *Phys. Rev. B* **35**, 7423 (1987).
- ²³E. Tosatti (private communication).
- ²⁴S. J. Vosko, L. Wilk, and M. Nusair, *Can. J. Phys.* **58**, 1200 (1980).
- ²⁵M. Büttiker, Y. Imry, R. Landauer, and S. Pinhas, *Phys. Rev. B* **31**, 6207 (1985).
- ²⁶D. M. Ceperley and B. J. Alder, *Phys. Rev. Lett.* **45**, 566 (1980).
- ²⁷J. Perdew and A. Zunger, *Phys. Rev. B* **23**, 5048 (1981).
- ²⁸G. B. Bachelet, D. R. Hamann, and M. Schlüter, *Phys. Rev. B* **26**, 4199 (1982).
- ²⁹A. Levy Yeyati, A. Martín-Rodero, and F. Flores, *Phys. Rev. B* **56**, 10 369 (1997).
- ³⁰R. Peierls, *Quantum Theory of Solids* (Clarendon Press, Oxford, 1955).
- ³¹E. Tekman and S. Ciraci, *Phys. Rev. B* **43**, 7145 (1991).
- ³²G. Rubio, N. Agraït, and S. Vieira, *Phys. Rev. Lett.* **76**, 2302 (1996).